Int. J. Environ. Res., 9(2):405-418, Spring 2015
ISSN: 1735-6865

Environmental Implications Related to Natural Asbestos Occurrences in the Ophiolites of the Gimigliano-Mount Reventino Unit (Calabria, Southern Italy)

Punturo, R.[1*], Bloise, A.[2], Critelli, T.[2], Catalano, M.[2], Fazio, E.[1] and Apollaro, C.[2]

[1]Dipartimento di Scienze Biologiche, Geologiche ed Ambientali - Università degli Studi di Catania, Corso Italia, 57, Catania, I-95129, Italy

[2]Dipartimento di Biologia, Ecologia e Scienze della Terra - Università della Calabria, Via Pietro Bucci, Cubo 15b, Rende, I-87036, Italy

Received 1 July 2014; Revised 28 Dec. 2014; Accepted 11 Jan. 2015

ABSTRACT: Metabasites and serpentinites of the ophiolitic sequence of the Gimigliano-Mount Reventino Unit (Calabria, southern Italy), also known as greenstones, are employed and marketed for building and ornamental purposes since prehistorical times. The main topic of our research focuses on the occurrence, within the above lithotypes, of asbestiform minerals that may be potentially harmful for human health. A detailed mineralogical and petrographic characterization by means of Polarized Light Microscopy (PLM), X-Ray Powder Diffractometry (XRPD), Scanning Electron Microscopy combined with Energy-Dispersive Spectrometry (SEM/EDS), and Thermo Gravimetry together with Differential Scanning Calorimetry (TG/DSC) pointed out as asbestiform minerals may occur in outcrops as well as in quarries located in surroundings of Mount Reventino. Indeed, tremolite resulted to be the main constituent among the asbestos minerals contained in metabasites, followed by actinolite; moreover, other amphiboles (not regulated by the Directive 2003/18/EC of the European Parliament and of the European Council of 27th March 2003) detected are crossite, glaucophane, hornblende and gedrite. As far as serpentinites, chrysotile is the dominant asbestos phase. Obtained results hold environmental implications, since they can be used in order to take decisions for the realization of health protecting measures during human activities such as road construction and quarry excavations and may also provide new data for the compulsory Italian mapping of natural sites that are characterized by the presence of the asbestos commonly known as NOA (Naturally Occurring Asbestos).

Key words: Naturally occurring asbestos, Greenstone, Metabasite, Serpentinite, Historical quarries, Calabria

INTRODUCTION

This study concerns the investigation of asbestiform amphibole and serpentine contained in the ophiolitic sequence belonging to the Gimigliano-Mount Reventino Unit (Sila Piccola, Calabria, southern Italy; Fig. 1a). This unit consists of metabasites (i.e., meta-basalts, gabbros and dolerites) and serpentinites with a metasedimentary cover made up of marble alternating with calc-schists and quartzites (Piluso *et al.*,2000; Liberi *et al.*, 2006; Barca *et al.*, 2010; Catalano *et al.*, 2014). A lot of literature is dedicated to the Calabrian ophiolites, dealing with the tectonic, petrological and geochemical features (Piccarreta & Zirpoli, 1969; Ogniben, 1973; Amodio Morelli *et al.*, 1976; Spadea, 1979; 1994; Beccaluva *et al.*, 1982; Morten & Tortorici, 1993; Piluso *et al.*, 2000; Alvarez, 2005; Pezzino *et al.*, 2008; Fazio *et al.*, 2008; Cirrincione *et al.*, 2008; 2010; Apollaro *et al.*, 2013). However, only a few works focus on the environmental aspects related to Natural Occurring Asbestos (NOA) and other fibrous minerals findings in the Calabrian ophiolites (e.g. Zakrzewska *et al.*, 2008; Campopiano *et al.*, 2009; Bloise *et al.*, 2012; Punturo *et al.*, 2013), or deal with their impact on human health (Pacella *et al.*, 2010; Bloise *et al.*, 2014).

Metabasites and serpentinites,also called greenstones, are employed and marketed as building and ornamental stones as well as for decorative jewels since pre-historical times (Punturo *et al.*, 2004; Zakrzewska *et al.*, 2008) because of their physical and mechanical properties; indeed, many historical quarries, which are either still active and abandoned, are spread in the area of Sila Piccola. Unfortunately, metabasites and serpentinites may contain asbestiform and other fibrous minerals. Owing to possible health problems due to asbestos fibre exposure (European

*Corresponding author E-mail: punturo@unict.it

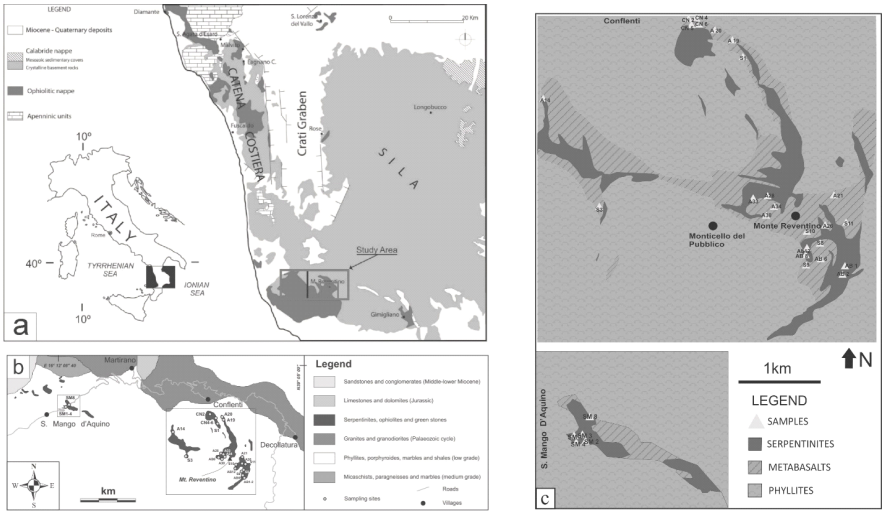

Fig.1. a) Geological sketch map of the northern sector of the Calabrian-Peloritani orogen, ophiolites occurrence and study area; b) Lithology of the study area and selected sampling sites; c) Detailed lithological maps of the sites; collected number samples are also plotted

Directive 2003/18/CE), the work in the greenstone quarries is regulated by the Italian law (DM 14/05/ 1996; DM 29/08/1999 and DM 25/07/2001). The regulated asbestos fibres (*i.e.*, chrysotile and amphiboles) correspond to fibres definite breathable by the WHO (World Health Organization), having length > 5 µm, width < 3 µm and ratio > 3. Several authors ascribe the fibres toxicity to their morphology and size, chemical-physical characteristics, surface reactivity and biopersistence (e.g.Mossman *et al.*, 2011). It is known that the presence of impurities (i.e., Fe, Ni, Ti) to ideal chemical composition in asbestos fibres, even in small amounts, affects their chemical and physical properties and size (Bloise *et al*., 2009a, b; Bloise *et al*., 2010); moreover, according to *in vitro* studies on biological system-mineral interactions, both characteristics (impurities and size) are considered to be responsible for the pathological effects (Fubini & Otero-Ar´ean 1999; Loreto *et al*., 2009; Pugnaloni *et al.*, 2013). For instance, studies focusing on the interactions between bronchoalveolar fluids and inhaled atmospheric particulate (Censi *et al*., 2011a, b), pointed out that, as a consequence of partial or total dissolution, metallic elements are released and accumulate in the human organs, inducing different health effects (Nordberg *et al*., 2007).

The univocal distinction between asbestiform *sensu strictu* and other fibrous minerals is that, even though these latter are not classified as "asbestos", may be potentially harmful to human health (*e.g.* Pugnaloni *et al*., 2013): i) is not so easy because some mineral fibres can be mistaken for asbestos and nevertheless ii) it is a matter of necessity because the Italian legislation demands the asbestos identification and quantification. Besides, the Italian law (DM 18/03/ 2003) requires to map out the natural occurrence of the asbestos in rocks in order to prevent people from the potential exposition to the asbestiform minerals.

In particular, about 7000 people living around the study area, which comprise the towns of Conflenti, Decollatura and San Mango D'Aquino together with their surroundings and near to Mount Reventino (Fig. 1), could be potentially exposed to asbestos risk due to the presence of historical quarries where the greenstones are exploited. Moreover, as asbestiform minerals can enter the soil and sediment through natural sources (e.g. weathering and erosion of asbestos-bearing rocks), the agricultural activities, through the plowing of the soil (Telloli *et al.*, 2014) can re-suspend such minerals thus increasing the amount of the fibres in the air. Previous studies on the asbestos presence, which are referred to the greenstone quarries (e.g. Campopiano *et al.*, 2009) highlighted the need to carry out detailed observations on fibrous amphiboles and other kind of fibrous minerals (e.g. the different varieties of amphiboles should be discriminated and characterized). More recently, Bloise *et al*. (2014) investigated the occurrence of asbestiform minerals in a suite of serpentinites from the Mount Reventino-Gimigliano Unit and detected fibrous minerals which could be potentially harmful for humans. In order to point out the eventual presence of asbestiform minerals within the metabasites of the ophiolitic sequence, and aiming to contribute for depicting a detailed distribution of the above minerals in a wide area of the Mount Reventino-Gimigliano surroundings, we carried out our investigation on both lithotypes of

interest (i.e. metabasites and serpentinites) on which the quarries (both active and inactive) sit (Fig. 1a-c).

MATERIALS & METHODS

The total extension of the study area, where the investigated ophiolitic sequences crop out, is close to 26 km^2 and comprises two historical quarries at Mt. Reventino and Conflenti-Decollatura surroundings, together with a road cut in the vicinity of the village of San Mango D'Aquino (Fig. 1a, b). The geology of Mt. Reventino area is characterised by an antiform that affects the whole ophiolitic sequence (Piluso et al., 2000). At the summit of Mt. Reventino, large lenses of massive and banded metabasalts as well as serpentinites are quite irregular in shape and display a complicated structure deformed into a pattern of tight folds (Alvarez, 2005). The serpentinites occupy the cores of the major folds and are partially or completely surrounded by isolated bodies of metabasalts (Fig.2a). Differently, in the Conflenti and Decollatura area, metabasites occur in large outcrops. The green colored rocks are present into two varieties: a foliated one and a massive one, respectively (Fig.2b, c). Serpentinites are dark green colored and crop out as massive bodies, sometimes weakly foliated, cut by serpentine (Fig.2d) and calcite veins. On the basis of the outcrop features and quarry occurrence, three sampling sites have been selected

Table 1. Studied localities, chilometric coordinates and, for each collected sample, mineralogical assemblage detected by XRPD, SEM–EDS, DSC–TG reported in order of decreasing abundance

Sample	Lithotype	Locality	Lon	Lat	Phases detected
SM2	Metabasite	San Mango D'Aquino- road cut	604420	4324593	Tr>Ctl>Atg
SM8	Metabasite	San Mango D'Aquino- road cut	604714	4324767	Tr>Act>Ctl>Chl
S1	Metabasite	Conflenti-Decollatura active quarry	612452	4323945	Chl>Ab>Di>Ms>Srp>Qtz>Tr>Ep
CN2	Metabasite	Conflenti-Decollatura active quarry	612355	4324469	Ab>Chl> Ms> Acmite-Augite>Glaucophane>Srp>Cal
CN4	Metabasite	Conflenti-Decollatura active quarry	612355	4324469	Ab>Ms>Chl>Acmite-Augite>Crossite>Qtz>Ctl>Cal
CN5	Metabasite	Conflenti-Decollatura active quarry	612355	4324469	Ms>Ab>Chl>Acmite-Augite>Ep>Crossite>Srp>Cal
CN6	Metabasite	Conflenti-Decollatura active quarry	612355	4324469	Ms>Ab>Chl>Acmite-Augite>Ep>Crossite>Srp>Cal
A19	Metabasite	Conflenti-Decollatura active quarry	612563	4324358	Chl>Ab>Ctl>Hbl
A20	Metabasite	Conflenti-Decollatura active quarry	612477	4324516	Chl>Ab>Ep>Ms>Act>Srp>Cal
A34	Metabasite	Mt Reventino surroundings	613540	4321114	Chl>Ab>Ms>Ep>Qtz>Act>Srp
A26	Metabasite	Mt Reventino surroundings	613821	4321875	Ab>Chl>Ep>Srp>Hbl
A28	Metabasite	Mt Reventino surroundings	613063	4322257	Ab>Chl>Act>Ep>Cal>>Ctl
S8	Metabasite	Mt Reventino surroundings	613653	4321583	Chl>Ab>Ttn>Ill>Tr>Ms>Srp
S9	Metabasite	Mt Reventino surroundings	613477	4321518	Ab>Chl>Tr>Ill>Ms>Ttn>Ep>Srp
A30	Metabasite	Mt Reventino surroundings	613116	4322689	Chl>Tr>Ctl>Ab>Ms>Tn>Ep
A21	Metabasite	Mt Reventino surroundings	612607	4322803	Chl>Ab>Ep>Ms>Cal>Srp>Act
S10	Metabasite	Mt Reventino surroundings	613585	4321848	Ab>Chl>Ms>Tr>Srp>Ep>Mag
S11	Metabasite	Mt Reventino surroundings	614101	4321894	Chl>Ab>Ms>Tr>Srp>Qtz>Ttn>Ep >Mag
A14	Metabasite	NW Mt Reventino	610119	4323457	Chl>Cal>Ged>Rt
S3	Metabasite	NW Mt Reventino	610945	4322051	Chl>Ab>Ms>Srp>Qtz>Act
AB6	Metabasite	Mt Reventino -inactive quarry	613703	4321481	Ab>Ms>Chl>Acmite-Augite>Ep>Crossite>Qtz>Ctl>Cal
AB12	Serpentinite	Mt Reventino -inactive quarry	613594	4321529	Ctl>Ant
R1	Ophicalcite	Mt Reventino -inactive quarry	613598	4321561	Cal>Srp
AB8	Ophicalcite	Mt Reventino -inactive quarry	613594	4321529	Cal>Srp
AB1	Serpentinite	Mt Reventino surroundings	614041	4321258	Lz> Ant> Ctl> Tr
AB2	Serpentinite	Mt Reventino surroundings	614041	4321258	Ctl> Ant> Liz>Chl>Ged
A33	Serpentinite	Mt Reventino surroundings	613587	4321226	Ctl> Lz> Atg>Chl>Cal
SM3	Serpentinite	San Mango D'Aquino- road cut	604420	4324593	Lz>Atg>Ctl
SM4	Serpentinite	San Mango D'Aquino- road cut	604420	4324593	Srp>Chl>Tr
SM1	Serpentinite	San Mango D'Aquino- road cut	604420	4324593	Ctl> Atg

Srp serpentine group minerals, *Atg* antigorite, *Lz* lizardite, *Ctl* chrysotile, *Tr* tremolite, *Di* diopside, *Mag* magnetite, *Chl* chlorite, *Ms* muscovite, *Ill* illite, *Ep* epidote, *Ab* albite, *Qtz* quartz, *Cal* calcite, *Rt* rutile, *Act* actinolite, *Ttn* titanite, *Hbl* hornblende, *Ged* gedrite (Mineral symbols after Kretz, 1983). *Acm-Aug* Acmite-Augite, *Crs* Crossite, *Gln* Glaucophane. *Regulated asbestos phases

after preliminary field work: the first one is located in the surroundings of the village of San Mango D'Aquino, where both metabasites and serpentinites are well exposed along a road cut; the second site is an active quarry close to the village of Conflenti and comprises metabasites; the third is in the area of Mt. Reventino and here both metabasites (Apollaro *et al.*, 2011) and serpentinites have been collected an abandoned quarry where serpentinite lithotype was formerly exploited has been investigated as well (Fig.1c; Table 1).

All samples were characterized by PLM, XRPD and SEM/EDS. X-ray powder diffraction patterns were obtained on a Bruker D8 Advance X-ray diffractometer with CuKα radiation, monochromated with a graphite monochromator at 40 kV and 40 mA. Scans were collected in the range of 3–66° 2θ, with a step interval of 0.02° 2θ and step-counting time of 3 seconds. EVA software (DIFFRACplus EVA) was used to identify the mineral phases in each X-ray powder spectrum, peaks being compared with 2005 PDF2 reference patterns.Secondary electron SEM imaging and microanalysis were performed on a FEI Quanta 200 equipped with a field emission gun (FEG) and equipped with an energy dispersive spectrometer (EDS). Part of the analyses were also performed on a Tescan-Vega\\LMU scanning electron microscope, equipped with an energy-dispersive X-ray spectrometer (EDS) Edax Neptune XM4 60, operating at 15 kV accelerating voltage and 20 nA beam current conditions. Thermogravimetric and differential scanning calorimetry (TG/DSC) was performed in an alumina crucible under a constant nitrogen flow of 30 cm^3min^{-1} with a Netzsch STA 449 C Jupiter in 25-1000 °C temperature range, and a heating rate of 10 °C/min. Instrumental precision was checked by repeated collections on a kaolinite reference sample (six collections), revealing good reproducibility (instrumental theoretical T precision of ± 1.2 °C) and theoretical weight sensitivity of 0.10 µg.

RESULTS & DISCUSSION

Metabasites show a main mineral assemblage given by chlorite, epidote, albite, amphibole (tremolite and Fe-actinolite ± glaucophane), quartz, white mica, calcite, titanite and opaque minerals, which define a grano-lepido-nematoblastic texture. These lithotypes are characterised by a compositional alternance between albite and epidote, ± quartz and calcite layers and by epidote, chlorite, amphibole and white mica levels (Fig. 3a). The average composition of metabasites occurring the study area is listed on Table 2. According to the literature (Piluso *et al.*, 2000; Punturo *et al.*, 2004; Liberi *et al.*, 2006), the geochemical features (e.g. SiO_2 *vs* Nb/Y content) of these metabasites suggest as the protolith was a sub-alkaline basaltic rock, with normalised patterns of High Field Strength (HFSE) and Rare Earth (REE) elements indicating transitional to enriched MORB affinity, as indicated in particular by some HFSEs (e.g. Zr, Hf, Ti, Y) and by the slight enrichment in light with respect to heavy REEs. Finally, it is worth noting that the abundances of K, La and Sr show evidence of sea-floor hydrothermal alteration as well as of ocean floor metamorphism followed by subsequent HP-LT metamorphism, as testified by the occurrence of Na-

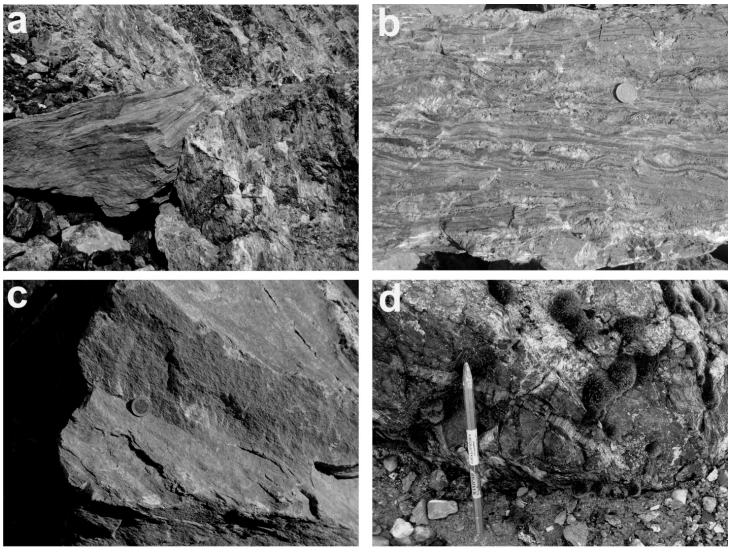

Fig. 2. a) Metabasite block within a large serpentinite body; b and c) foliated and massive metabasite varieties, respectively; d) massive serpentinite body with serpentine vein

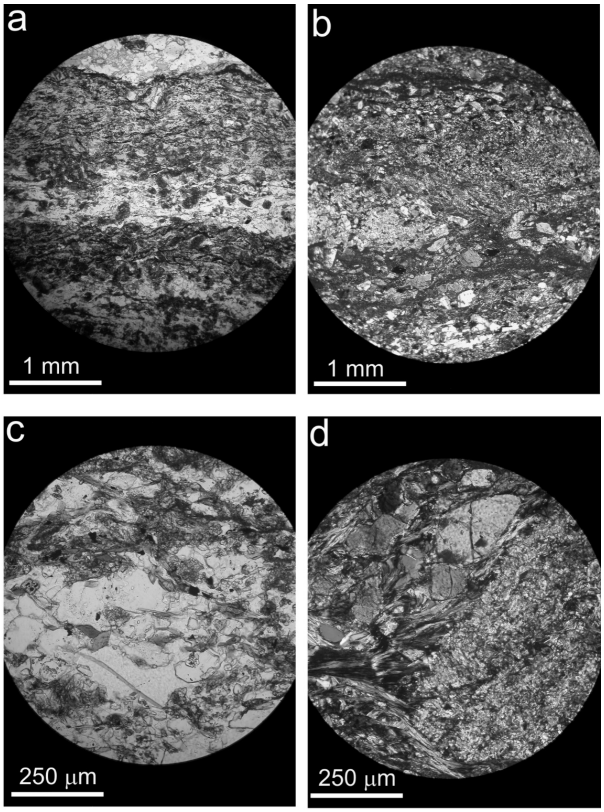

Fig. 3. Photomicrographs of: a) Foliated metabasite (plain polarized light), with granoblastic (albite, epidote, quartz and calcite) and lepido-nematoblastic (epidote, chlorite, amphibole and white mica) layers; b) Large prismatic epidote together with smaller rounded individuals (crossed polarizers); c) Acicular to fibrous amphibole. The picture shows the glaucophane-rich variety (plain polarized light); d) Detail of an epidote-rich layer: larger grains are embedded with chlorite and small amounts of amphibole and white mica. To the right, small sub-idioblastic epidote aggregates occur

amphibole; finally, a retrograde event under low grade greenschist facies conditions is indicated by the association of chlorite, epidote, albite and tremolite-actinolite (Piluso *et al*., 2000). As far as the mineral assemblage, epidote is the most abundant phase. It occurs as prismatic to sub-idioblastic crystals; zoning is sometimes present. Prismatic crystals are relatively larger than rounded grains, which usually occur as aggregates (Fig. 3b). Epidote ranges in color from pale yellow to green; the brownish variety may be also present. Chlorite (nα=colorless; nγH"nβ=pale green) is mainly present in association with amphibole and epidote (Fig. 3c, d), even though it may also occur as isolated crystals within the quartz-albite rich domains. Albite constitutes, together with epidote and minor xenoblastic quartz and calcite, the granoblastic domains (Fig. 3c). Amphibole, which shows chlorite intergrowths, is mainly tremolite and Fe actinolite, weakly pleochroic from colorless to pale green (Fig. 3a) and usually occurring as acicular and fibrous crystals. It is worth noting that in the quarry near to Conflenti village, acicular and prismatic Na-amphibole (nα=colorless, nβ= lavender blue, nγ=blue) has been found within both nematoblastic and granoblastic domains, sometimes also occurring as fibrous crystals (Fig. 3c). Finally, titanite is present as small crystals oriented within the main foliation plane. The serpentinites and ophicalcites show remnants of the original protogranular texture, which has been inherited from their harzburgitic-lherzolitic protoliths. According to the available literature data (cfr. Punturo *et al.*, 2004; Liberi *et al*., 2006) they show Al_2O_3 as well as MgO and Cr contents, considered to be unmodified after serpentinization, comparable with less depleted oceanic peridotite (Bonatti & Michael, 1989; Niu, 2004), as also revealed by incompatible and rare earth elements patterns (Punturo *et al.*, 2004). The average composition of serpentinite from the Mt. Reventino area, where the quarries occur, is set out in Table 2. The mineral assemblage is, on the whole, made of serpentine group minerals and magnetite ± tremolite-actinolite ± chlorite ± clinopyroxene ± Cr-spinel and calcite (this latter abundant in the two ophicalcite samples). The serpentine group minerals and small magnetite grains

Table 2. Average major (wt%) and trace elements (ppm) of serpentinites, metabasites and ophicalcites of the study area (values compiled after Punturo *et al.*. 2004 and Liberi *et al.*. 2006); *n*= number of analyses; b.d.=below detection limits

	Serpentinite	Metabasite	Ophicalcite
	Mean (n=10)	*Mean (n=15)*	*Mean (n=3)*
wt%			
SiO_2	39.51	44.35	37.44
TiO_2	0.04	1.90	0.03
Al_2O_3	1.97	12.9	1.48
Fe_2O_3	7.12	11.3	8.48
MnO	0.08	0.19	2.34
MgO	38.57	9.48	39.43
CaO	0.45	11.0	4.11
Na_2O	b.d	2.70	b.d.
K_2O	b.d.	0.57	b.d
P_2O_5	0.01	0.19	b.d.
L.O.I.	12.70	5.45	13.77
ppm			
Y	11	35	11
Nb	0.4	4	0.84
La	8	8	19.62
Ce	15	21	30.39
Pr	0.3	3	
Nd	1	14	
Sm	0.2	4	
Eu	0.1	2	
Gd	0.3	6	
Tb	0.1	1	
Dy	0.3	6	
Ho	0.1	1	
Er	0.2	4	
Tm	0.0	1	
Yb	0.3	3	
Lu	0.1	b.d.	
Cr	2691	236	2463
Ni	1982	129	1876
Rb	3	14	8
Ba	17	25	8
Hf	2	3	
Ta	0.4	b.d.	
Pb	12	b.d.	
Th	0.1	b.d.	0.4
U	0.1	b.d.	
Sc	11	35	
V	52	219	47
Co	107	33	94
Sr	6	145	16
Zr	27	124	
Zn	62	76	

completely replaced the original olivine and orthopyroxene crystals and appear as pseudomorphic aggregates with typical net-like and mesh textures (Fig. 4a,b). Different dilatation vein systems, filled by serpentine group minerals cross-cut the rock (Fig. 4c, f). In general, serpentine fibres may be oriented either perpendicular to the vein selvages ("cross" serpentine) or according to their elongation directions ("lamellar" serpentine; see Fig.4 a, c, e, f). The medium line of the vein is often marked by small magnetite grains (Fig. 4c); moreover, calcite and talc flake aggregates or actinolite-tremolite fibres may in part fill the veins or occur within the serpentine matrix (Fig.4d). Orthopyroxene grains appear deeply replaced by "bastite", whereas clinopyroxene has been observed as millimetric grains or inclusions within the rarely preserved holly-leaf shaped Cr-spinels of peridotitic origin (Fig. 4a) that, in most cases, are quite completely retrogressed to magnetite and chlorite.

Finally, the ophicalcite bands found in the inactive quarry of Mt. Reventino exhibit a brecciated fabric, with mineralogical assemblage given by calcite and serpentine ± chlorite, tremolite and magnetite (average composition set out on Table 2).

X-ray diffraction data from metabasalt and serpentinite samples are reported in Table 1. Results show that the mineral assemblages in almost all samples of metabasites rocks contains (in order of decreasing abundance) chlorite, albite, epidote, amphiboles, serpentine minerals, quartz and micas. Calcite was also detected in variable proportions but not in all samples, while among the subordinate phases, titanite and magnetite were the most frequent. The XRPD pattern clearly indicates that tremolite-actinolite are the dominant phases (see Table 1); all amphiboles were further characterized by their EDS spectrum.With regard to serpentinitic rocks (Table 1), serpentine minerals dominate all the samples, followed by chlorite and tremolite (in three out of seven samples). Calcite was detected less frequently (in sample A33) and in low amount. Although the XRPD method used does not allow the polytypes of the serpentine phases to be specified accurately because their peaks appear at nearly the same position, the position of the main peak, which is related to the chemical composition of serpentine, could give some information about the type of analyzed mineral (Wicks & O'Hanley, 1988). However, for a detailed identification and semi-quantitative amount of the serpentine minerals, other specific techniques as TG/DSC analyses must be made. Such detailed mineralogical analyses on both metabasalts and serpentinite samples are reported below. Morphological observations combined with EDS chemical analyses show that amphibole (both tremolite and actinolite) fibres appear thin and rigid (Fig. 5 a-d). As far as serpentine group minerals, chrysotile shows the classical curved cylindrical fibres whereas lizardite exhibits only plate-like morphology and antigorite is characterized by lamellar shape (Fig.6 a, b). Chrysotile fibres (formed by curved scrolls and/or hollow cylinders), are often arranged in parallel strands (Fig. 6 c, d); at a more detailed scale, it is evident that chrysotile threads form bundles several microns long (Fig.6 e,f). Data on analyzed samples reveal that these fibres show a size that, according to several authors (Bernstein *et al.*, 2005; Stanton *et al.*, 1981;

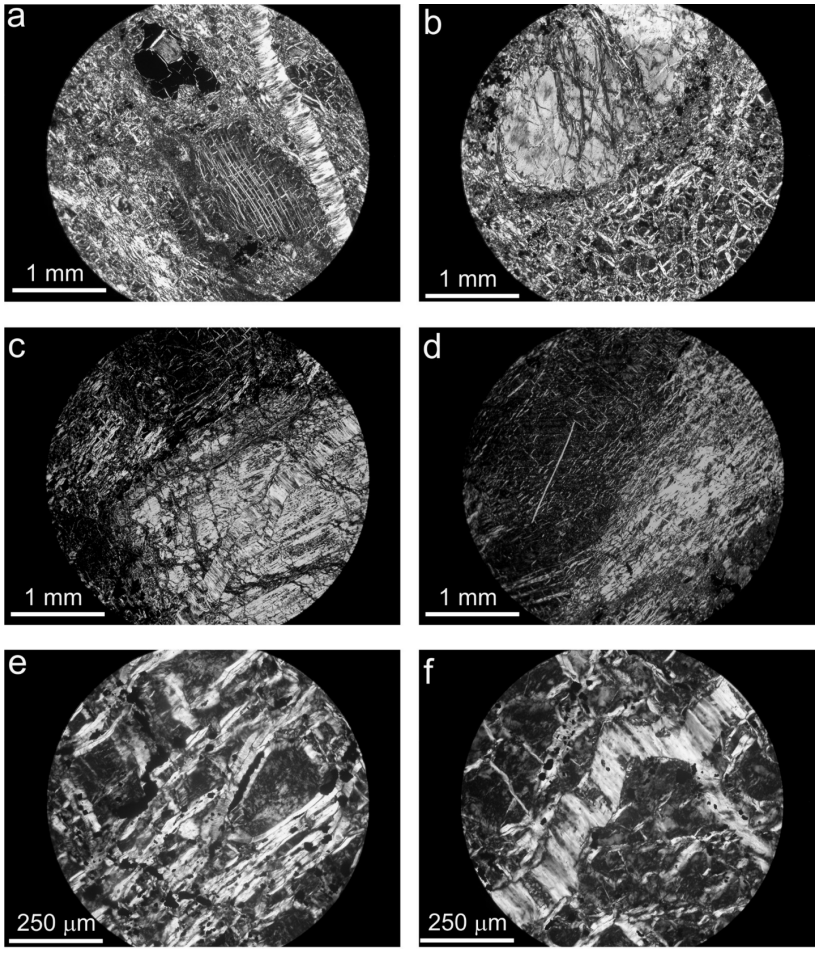

Fig.4. Photomicrographs of: a) Top left. Relic of holly-leaf shaped spinel enclosing former clinopyroxene, large olivine pseudomorph is also present, together with cross-serpentine vein; b) Large orthopyroxene pseudomorph within mesh serpentine matrix; c) Dilatation vein system, cutting the serpentine matrix; d) Slip serpentine (right) and (to the left) one actinolite/tremolite fibre evident; e) Detail of mesh serpentine, with secondary magnetite and small relics of pyroxene; f) Detail of cross-serpentine vein together with secondary magnetite. All photomicrographs taken at crossed polarizers conditions

Berman *et al.*, 1995), may be significantly associated with carcinogenesis when breathed.

It is important to point out that this kind of fibres dimension could become shorter after excavation works or because they tend to split up along their elongation axis (Figs.5b,d; 6c); Loomis *et al.*, 2010; Dodson *et al.*, 2003 and Suzuki *et al.*, 2005 have reported that fibres shorter than 1.5 μm could also be further associated with carcinogenic lung cancer.Finally, it is difficult to evaluate within serpentinites the amount of each fibrous phase by SEM since amphiboles with asbestiform habit are typically intergrown with serpentine minerals.

Each variety of serpentine minerals and fibrous amphiboles has been chemically analyzed to complete their characterization or, in certain cases, to solve the identification. Six different types of amphiboles have been mainly recognized: they are mainly tremolite, actinolite, with minor hornblende, gedrite, crossite and glaucophane. These varieties, which may also coexhist in the same rock, testify the complex metamorphic history that ophiolite experienced from ocean floor to HP-LT metamorphism to greenschist facies conditions last episode. Asbestos amphiboles (actinolite-tremolite) classification are shown graphically in Fig. 7 and their chemical compositions are listed in Table 3. Hornblende and gedrite were found less frequently and their chemical formula, written on the basis of 23 oxygen is $Na_{0.32}Ca_{1.40}(Mg_{3.49}Fe_{1.51})[(Al_{0.57}Si_{7.41})O_{22}]OH_2$ and $Na_{0.19}(Ca_{0.88}Mg_{4.26})(Mg_{1.03}Fe_{0.79}Al_{0.18}Ti_{0.04})[(Al_{1.56}Si_{6.44})O_{22}]\ OH_2$, respectively. Na amphibole is rare and has a crossitic-glaucophane composition.

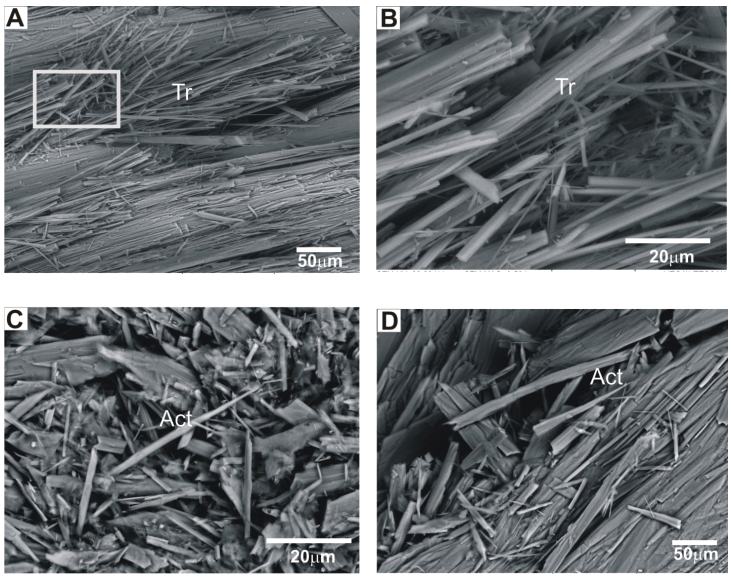

Fig.5. Secondary electron SEM images of: a) asbestos tremolite, the rectangle indicates the position of b), showing the splitting of fibres along their elongation direction; c) actinolite needles, which can break into smaller sized fibres (d). Mineral symbols as in Table 1

Table 3. Average compositions of asbestiform amphiboles detected in metabasites and serpentinites

Samples	SM2	A34	SM8		A20	A28	A30	
Oxides wt%	Tr	Act	Tr	Act	Act	Act	Tr	Act
SiO_2	57.41	57.21	60.28	58.70	54.24	55.39	58.93	54.96
TiO_2	0.00	0.00	0.00	0.00	0.00	0.00	0.00	0
Al_2O_3	1.46	2.95	0.41	0.66	3.70	2.53	2.16	2.21
FeO	3.27	10.72	3.32	9.59	13.84	12.45	9.61	14.08
MnO	0.00	0.00	0.00	0.00	0.00	0.46	0.24	0.00
MgO	27.11	16.76	23.31	17.86	14.34	16.63	18.53	16.17
CaO	10.74	11.11	11.89	12.43	12.25	10.91	7.98	11.43
Na_2O	0.00	1.24	0.80	0.77	1.63	1.63	2.56	1.15
Total	100	100	100	100	100	100	100	100
CATIONS calculated on the basis of 23 oxygens								
Si	7.61	7.86	7.98	8.07	7.67	7.66	7.87	7.65
Al^{IV}	0.23	0.14	0.02	0.00	0.33	0.34	0.13	0.35
Al^{VI}	0.00	0.34	0.05	0.11	0.28	0.07	0.21	0.01
Ti	0.00	0.00	0.00	0.00	0.00	0.00	0.00	0.00
Cr	0.00	0.00	0.00	0.00	0.00	0.00	0.00	0.00
Fe^{3+}	0.36	0.20	0.37	0.00	0.00	0.59	0.97	0.63
Fe^{2+}	0.00	1.03	0.00	1.10	1.64	0.85	0.10	1.01
Mn	0.00	0.00	0.00	0.00	0.00	0.05	0.03	0.00
Mg	5.36	3.43	4.60	3.66	3.02	3.43	3.69	3.35
Ca	1.53	1.64	1.69	1.83	1.86	1.62	1.14	1.70
Na	0.00	0.33	0.21	0.21	0.45	0.44	0.66	0.31

EDS/SEM analyses revealed a few percent replacement of Si for Al, Mg for Fe, and low replacements of Al for the Mg in the octahedral sites in the serpentine minerals. In some samples, low amounts of Cr were also detected. The representative chemical formula for asbestos chrysotile is $(Mg_{2.48}Fe_{0.12}Ca_{0.02}Cr_{0.03}Al_{0.27})(Si_{2.87}Al_{0.13})O_5(OH)_4$.

Thermal analysis has been successfully employed in serpentine polymorphs distinction (antigorite, lizardite, chrysotile). TG analyses for serpentinites show total weight losses of 12–14 % at 1000 °C in all samples (Table 4), in agreement with the theoretical structural water content in serpentine (Roveri *et al.*, 2006; Viti, 2010; Viti *et al.*, 2011; Bloise *et al.*, 2014). Fig. 8a shows some general features shared by all serpentinites which allowed to define the temperature ranges reported in Table 3, such as: i) very limited weight loss (1–3 %) below 600 °C (Fig. 6a, dashed line) which represents the starting temperature of the main loss episode; ii) marked weight loss in the 600–800 °C range (Fig. 8a, dashed line); and iii) the occurrence of a sharp exothermic DSC signal, systematically close to 820 °C (Table 4; Fig. 8a, solid line) which represents the end of the main loss episode.

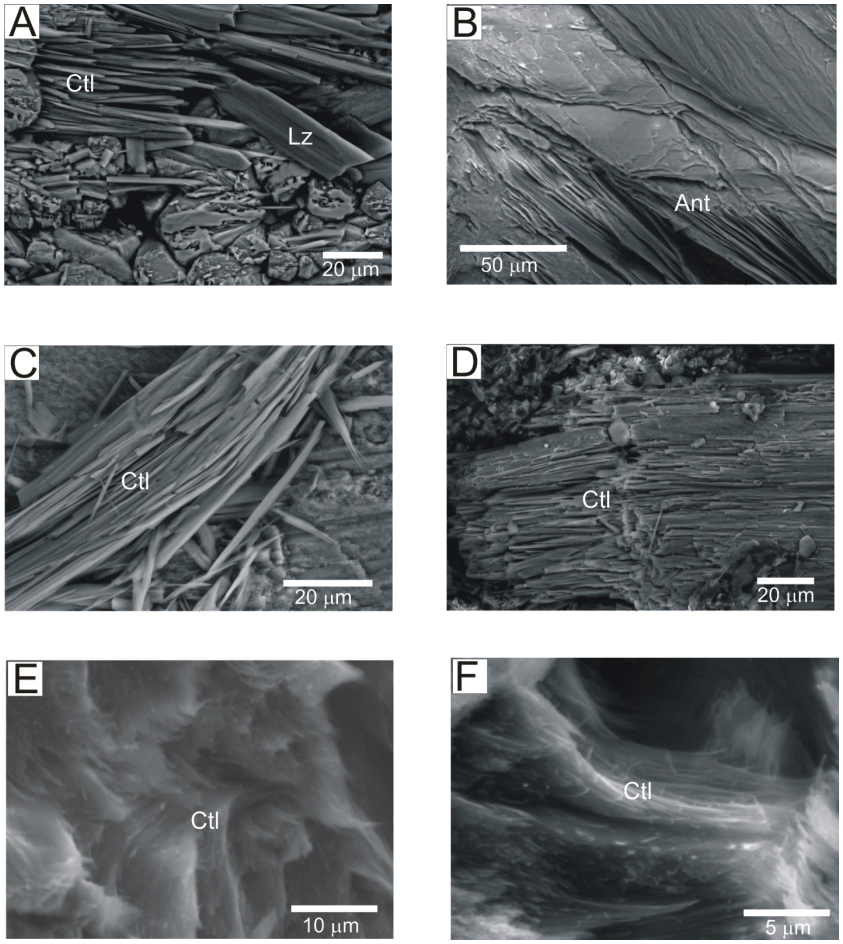

Fig.6. Secondary electron SEM images of serpentine group minerals: a) Elongated chrysotile and platy lizardite; b) Lamellar antigorite; c) Chrysotile hollow cylinders, which are often arranged into d) parallel strands; e) Curved chrysotile fibres; f) Chrysotile longitudinal splitting into thinner fibrils from larger fibre. Mineral symbols as in Table 1

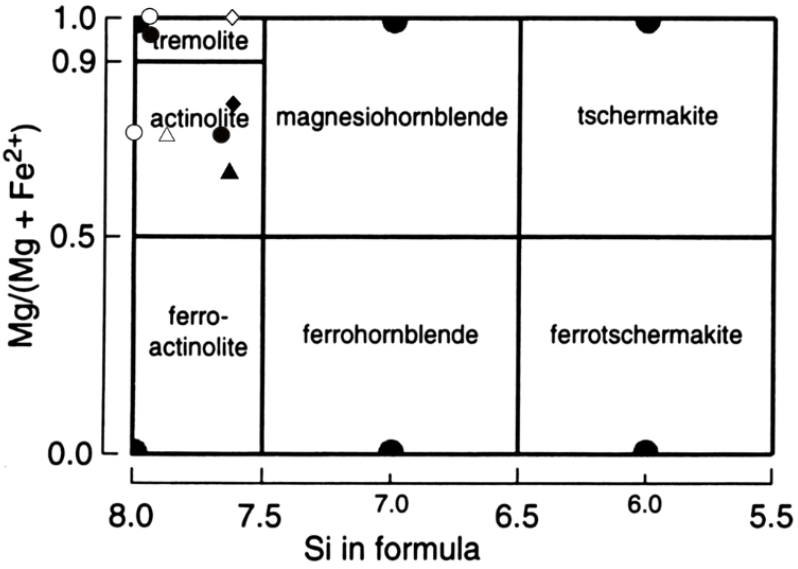

Fig.7. Classification diagram for the calcic amphiboles (fields after Leake *et al.*, 1997)

Table 4. Main TG data for (weight loss %) for AB1, AB2, AB12, SM1, SM3, A33 and SM4 samples.

AB1		**AB2**	
T range (°C)	TG loss %	T range (°C)	TG loss %
25-641,5	2.31	25-616,3	4.26
641,5-779,8	9.06	616,3-687,9	5.56
779,8-820,8	0.62	687,9-818,4	2.35
sum at 820.8	11.99	sum at 818,4	12.17
tot loss at 1000	12.47	tot loss at 1000	12.42
AB12		**SM1**	
25,616,6	2.63	25-615,6	3.11
616,6-665,7	3.26	615,6-760,6	9.12
665,7-770	5.24	760,6-820,3	0.82
770-820,3	0.83	-	-
sum at 820,3	11.96	sum at 820.3	13.05
tot loss at 1000	12.25	tot loss at 1000	13.41
SM3		**A33**	
25-624,2	1.47	25-606.1	3.43
624,2-768,9	9.46	606.1-755.4	8.47
768,9-822	0.87		
-	-		
sum at 822	11.8	sum at 755.4	11.9
tot loss at 1000	12.2	tot loss at 1000	13.05
SM4			
25-615,3	2.43		
615.3-780,1	8.96		
780.1-821.5	0.73		
-	-		
sum at 821.5	12.12		
tot loss at 1000	13.01		

Note: the meaning of *T* ranges (first column for each sample) is explained in the text.

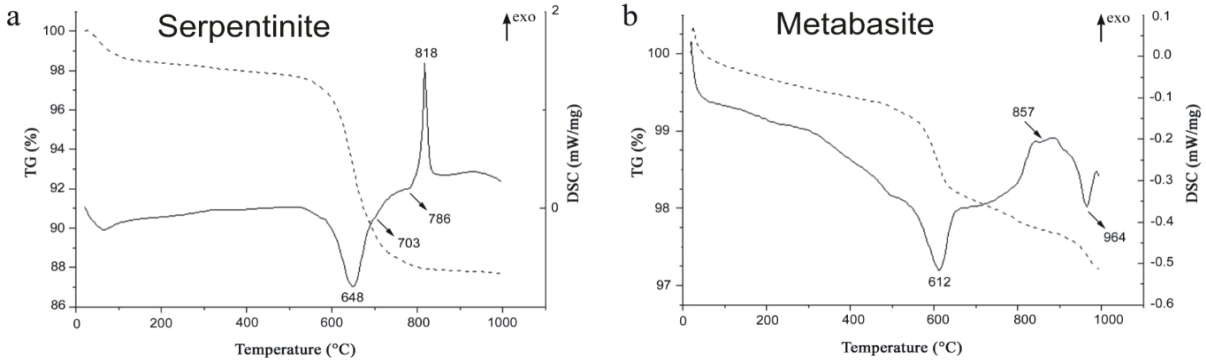

Fig. 8. Typical DSC (solid line) and TG (dashed line) curves of: a) serpentinite (specimen AB2) and b) metabasite (specimen A30), representing the behaviour of the studied lithotypes

The DSC patterns for all the serpentinitic samples show a main peak in a temperature range 625.5-651.6 °C (Fig. 8a, solid line), linked to chrysotile breakdown.

Antigorite is present in all samples as shown by the presence of an endothermic peak in a temperature range of 715-786.6 °C. In particular, samples SM1, SM4, A33, SM3 and AB12 are characterized by an

Table 5. Peak temperatures in DSC curves for AB1, AB2, AB12, SM1, SM3, A33 and SM4 samples

AB1	AB2	AB12	SM1	SM3	A33	SM4
			DSC			
633.4 endo w sh						
677.3 endo w sh	648.9 endo ss	651.6 endo ss	649.4 endo ss	633.9 endo w	643.1 endo ss	652.3 endo w
710.7 endo ss	703 endo sh	719.4 endo sh	718.4 endo	700.4 endo ss	699.3 endo w	715.2 endo sh
749 endo				736.7 endo s	731.1 endo w	
807.4 endo w sh	786.6 endo w	778.8 endo sh		807 endo sh		
820.8 exo ss	818.4 exo	820.3 exo	819 exo	822 exo ss	822.8 exo ss	821.5 exo

Note : w = weak, s = strong, ss = very strong (main peak), sh = shoulder; endo = endothermic, exo = exothermic.

endothermic peak at 718.4 °C, 715.2 °C, 731.1 °C, 736.7 °C and 719.4 °C, respectively. In samples AB1, AB2 and AB12 the presence of antigorite is confirmed by its diagnostic high-T-peak at 749 °C, 786.6°C, and 778.8 °C, respectively. Lizardite is present in four samples (AB1, AB2, A33, SM3) as indicated by the occurrence of an endothermic peak in a temperature range of 698.6-710.7 °C. A sharp exothermic peak is shown at 818-826°C in all the samples which indicates the crystallization of forsterite (Bloise *et al.*, 2009a,b,c; 2010).

The interpretation of TG/DSC data on metabasite samples is more complicated since these rocks contain various minerals (see XRPD and petrography sections). Nevertheless, we focused on the identification of fibrous phases (i.e. serpentine minerals and amphiboles); as an example of TG/DSC patterns of metabasite, we report the results of specimen A30 (Fig. 8b). In particular, it has been observed that samples A30, A28, A34, CN4, A19, SM8 and A14 show an endothermic peak in a temperature range of 591.3-656.7 °C (Fig. 8b, solid line). The presence of this peak has been interpreted as due to chrysotile break down even if the T range is lower than the one found by Bloise *et al*. (2014). The difference in the thermal range may be assigned to the presence of high iron contents that induce a shift to lower temperature of the endothermic area (Foresti *et al*., 2005). Sample SM2 shows a weak endothermic peak at 714.3 °C ascribed to antigorite. The characteristic endothermic peak of amphibole asbestos has been found in almost all samples. The weak endothermic peak found in samples A30, A34 and A19 in a thermal range of 818.5-857.9 °C, and a strong endothermic peak recognized at 964.6 °C and 967.5 °C in samples A30 and A34, respectively (Fig. 8b, solid line), can be associated to tremolite (Bloise *et al.*, 2008) and to actinolite (Belyankin and Donskaya, 1939; Vermaas, 1952; Dostal, 1965).

CONCLUSIONS

In the ophiolite sequence which crops out in the surroundings of Mt Reventino (Calabria, southern Italy), asbestiform tremolite is the main constituent of metabasites followed by minor actinolite that becomes more abundant in the metabasite collected at San Mango D'Aquino road cut whereas, in the active quarry of Conflenti-Decollatura, tremolite occurs together with glaucophane. Other amphiboles (not asbestiform) have been detected according to the following decreasing abundance: crossite, glaucophane, hornblende and gedrite. Some rare chrysotile fibres have been also detected within metabasite lithotypes that crop out in the surroundings of Mt. Reventino. Asbestiform tremolite has also been detected within the serpentinites together with asbestiform chrysotile, which is the dominant phase among the serpentine group minerals. Results emerged from the present study indicate that, when in the main lithotypes that constitute the ophiolitic sequence of Mt. Reventino- Gimigliano Unit, amphiboles and serpentine group minerals may also crystallize with asbestiform habit (i.e., according to WHO: length > 5 µm, width < 3 µm and ratio > 3; see Figs. 4d, 5 and 6); if this is the case, they become potentially harmful. For the above reason, greenstones should be carefully scrutinized before their employment as building or construction materials and, to this aim, the role of geoscientists is crucial in guiding safe rock extraction. This new knowledge besides the data from Bloise *et al*. (2014) improve the Italian mapping of natural sites characterized by the presence of asbestos minerals, with particular regards to the ophiolitic sequences which crop out in Calabria. Furthermore, they can be used in order to assess the health risks related to the exposure to NOA during human activities, such as road construction, quarry excavations and farming that may induce disturbance in the asbestos-bearing rocks and trigger unplanned asbestos release process.

ACKNOWLEDGEMENTS

The authors grateful to Rosolino Cirrincione for his valuable help during the sample collection and for the fruitful discussions on the Calabrian ophiolites and to Carmela Vaccaro for her constructive review.The research was partially funded by the University of Catania – Researchers' fundings 2012.

REFERENCES

Alvarez, W. (2005). Structure of the Mount Reventino greenschist folds: a contribution to untangling the tectonic-transport history of Calabria, a key element in Italian tectonics. - J. Struct. Geol. **27 (8),** 1355-1378.

Amodio Morelli, L., Bonardi, G. and Colonna, V. (1976). L'Arco calabro-peloritano nell'orogene Appenninico - Maghrebide. - Memorie della Società Geologica Italiana **17 (1),** 60.

Apollaro, C., Marini, L., Critelli, T., De Rosa, R., Bloise, A., Miriello, D., Catalano M. and Armano V. (2013). Modeling of the impact of dolomite and biotite dissolution on vermiculite composition in a gneissic shallow aquifer of the Sila Massif (Calabria, Italy). - Appl. Geochem. **35,** 297-311.

Apollaro, C., Marini, L., Critelli, T., Barca, D., Bloise, A., De Rosa, R., Liberi, F. and Miriello D. (2011). Investigation of rock-to-water release and fate of major, minor, and trace elements in metabasalt –serpentinite shallow aquifer of Mt. Reventino (CZ, Italy) by reaction path modelling. - Appl. Geochem., **26,** 1722–1740. (CZ, Italy) by reaction path modelling

Barca, D., Cirrincione, R., De Vuono, E., Fiannacca, P., Ietto, F., and Lo Giudice, A. (2010). The Triassic rift system in the northern calabrian-peloritani orogen: Evidence from basaltic dyke magmatism in the San Donato unit. - Periodico Di Mineralogia, 79 (2), 61-72.

Beccaluva, L., Maciotta, G. and Spadea, P. (1982). Petrology and geodynamic significance of the Calabria– Lucania ophiolites. - Rendiconti Società Italiana di Mineralogia e Petrologia **38,** 973–87.

Belyankin, D.S. and Donskaya, E.V. (1939). Thermo-optical investigation of actinolite. - Acd. Sci. U.R.S.S. Bull. 1, 95-104 (in Russian with English summary).

Berman, D.W., Crump, K.S., Chatfield, E.J., Davis, J.M.G. and Jones, A.D. (1995). The sizes, shapes, and mineralogy of asbestos structures that induce lung tumors or mesothelioma in AF/HAN rats following inhalation. - Risk Anal **15(2),** 181–195.

Bernstein, D., Castranova, V., Donaldson, K., Fubini, B., Hadley, J., Hesterberg, T., Kane, A., Lai, D., McConnell, E.E., Muhle. H., Oberdorster, G., Olin, S., and Warheit, D.B. (2005). Testing of fibrous particles: short-term assays and strategies. - Inhal.Toxicol. **17,** 497–537.

Bloise, A., Fornero, E., Belluso, E.,Barrese, E., Rinaudo, C. (2008). Synthesis and characterization of tremolite asbestos fibres. -Eur. J. Mineral. **20**, 1027–33.

Bloise, A., Barrese, E. and Apollaro, C. (2009 a). Hydrothermal alteration of Ti-doped forsterite to chrysotile and characterization of the resulting chrysotile fibres. - N. Jb. Miner Mh **185 (3),** 297-304.

Bloise, A., Belluso, E., Barrese, E., Miriello, D. and Apollaro, C. (2009b). Synthesis of Fe-doped chrysotile and characterization of the resulting chrysotile fibers. - Cryst. Res. Technol. **44 (6),** 590–596.

Bloise, A., Barrese, E., Apollaro, C. and Miriello, D. (2009c). Flux growth and characterization of Ti- and Ni-doped forsterite single crystals. - Cryst. Res. Technol., **44,** 463-468.

Bloise, A., Belluso, E., Fornero, E., Rinaudo, C., Barrese, E. and Capella, S. (2010). Influence of synthesis condition on growth of Ni-doped chrysotile. - Microporous Mesoporous Mater **132,** 239–245.

Bloise, A., Belluso, E., Critelli, T., Catalano, M., Apollaro, C., Miriello, D. and Barrese, E. (2012). Amphibole asbestos and other fibrous minerals in the meta-basalt of the Gimigliano-Mount Reventino Unit (Calabria, south-Italy). - Rend. Online Soc. Geol. It. **21(2),** 847–848.

Bloise, A., Critelli, T., Catalano, M., Apollaro, C., Miriello, D., Croce, A., Barrese, E., Liberi, F., Piluso, E., Rinaudo, C. and Belluso, E. (2014). Asbestos and other fibrous minerals contained in the serpentinites of the Gimigliano-Mount Reventino unit (Calabria, S-Italy). - Environmental Earth Sciences, **71(8),** 3773-3786.

Bonatti, E. and Michael, PJ., (1989). Mantle peridotites from continental rifts to ocean basins to subduction zones. - Earth Planet. Sci. Lett., **91,** 297-311.

Campopiano, A., Olori, A., Zakrzewska, A.M., Capone, P.P. and Iannò A. (2009). Chemical-mineralogical characterisation of greenstone from San Mango d'Aquino. - Prev. Today **5(3/4),** 25–38.

Catalano, M., Bloise, A., Miriello, D., Apollaro, C., Critelli, T., Muto, F., Cazzanelli, E. and Barrese, E. (2014). The mineralogical study of the Sant'Angelo Inferiore cave (southern italy). - Journal of Cave and Karst Studies, **76 (1),** 51–61.

Censi, P., Tamburo, E., Speziale, S., Zuddas, P., Randazzo, L. A., Punturo, R., Cuttitta A. and Aricò, P. (2011). Yttrium and lanthanides in human lung fluids, probing the exposure to atmospheric fallout. - Journal of Hazardous Materials, **186(2-3),** 1103-1110.

Censi, P., Zuddas, P., Randazzo, L. A., Tamburo, E., Speziale, S., Cuttitta, A., Punturo., R., Aricò, P. and Santagata, R. (2011). Source and nature of inhaled atmospheric dust from trace element analyses of human bronchial fluids. - Environmental Science and Technology, **45(15),** 6262-6267.

Cirrincione, R., Fazio, E., Heilbronner, R., Kern, H., Mengel, K., Ortolano, G., Pezzino, A. and Punturo R. (2010). Microstructure and elastic anisotropy of naturally deformed leucogneiss from a shear zone in Montalto (southern Calabria, Italy). – Geol. Soc. London, Spec. Publications, **332,** 49-68.

Cirrincione, R., Fazio, E., Fiannacca, P., Ortolano, G., Pezzino, A. and Punturo, R. (2008): Petrological and microstructural constraints for orogenetic exhumation modelling of HP rocks: th example of southern Calabria Peloritani Orogen (western Mediterranean). In: Third international Geomodelling conference, 22-24 september 2008, Firenze. - Boll. Geofisica Teorica ed Applicata, **49,** 141-146.

Dodson, R.F., Atkinson, M.A. and Levin J.L. (2003), Asbestos fiber length as related to potential pathogenicity: a critical review. - Am. J. Ind. Med. **44,** 291–297.

Dostal, J. (1965). Mineralogical and chemical investigation of actinolite from Sobotin, Czechoslovakiaj. - Acta Univ. Carolinea- Geologica, **3,** 175-188 (Russian and English Summaries).

Fazio, E., Cirrincione, R. and Pezzino, A. (2008). Estimating P-T conditions of Alpine-type metamorphism using multistage garnet in the tectonic windows of the Cardeto area (southern Aspromonte Massif, Calabria). - Mineralogy and Petrology, **93,** 111-142.

Foresti, E., Hochella, M.F., Lesci, I.G., Madden, A.S., Roveri, N. and Xu H (2005). Morphological and chemical/physical characterization of Fe-doped synthetic chrysotyle nanotubes. - Adv. Funct. Mater. **15,** 1009-1016.

Fubini, B. and Otero, A.C. (1999). Chemical aspects of the toxicity of inhaled mineral dusts. - Chem. Soc. Rev. **28,** 373–383.

Kretz, R. (1983). Symbols for rock-forming minerals. - American Mineralogist, **68,** 277-279.

Leake B.E. et al., (1997). Nomenclature of amphiboles: report of the subcommittee on amphiboles of the international mineralogical association, commission on new minerals and mineral names. - The Canadian Mineralogist, **35,** 219-246.

Liberi, F., Morten, L. and Piluso, E. (2006). Geodynamic significance of ophiolites within the Calabrian Arc. Island Arc, **15,** 26-43.

Loomis, D., Dement, J., Richardson, D. and Wolf, S. (2010). Asbestos fibre dimensions and lung cancer mortality among workers exposed to chrysotile. - Occup. Environ. Med. **67(9),** 580–584.

Loreto, C., Carnazza, M.L., Cardile, V., Libra, M., Lombardo, L., Malaponte, G., Martinez, G., Musumeci, G., Papa, V. and Cocco, L. (2009), Mineral fiber-mediated activation of phosphoinositide-specific phospho- lipase c in human bronchoalveolar carcinoma-derived alveolar epithelial A549 cells. - Int. J. Oncol. **34,** 371–376.

Morten, L. and Tortorici, L. (1993). Geological framework of the ophiolite-bearing allochtonous terranes of the calabrian arc and lucanian apennines. in: italian eclogites and related rocks. (L. Morten ed.). - Accademia Nazionale delle Scienze detta dei Xl, **13,** 145-150.

Mossman, B.T., Lippmann, M., Hesterberg, T.W., Kelsey, K.T., Barchow-sky, A., Bonner, J.C. (2011). Pulmonary endpoints (lung carcinomas and asbestosis) following inhalation exposure to asbestos. - J. Toxicol. Environ. Health B 14(1–4), 76–121.

Niu, Y. (2004). Bulk-rock major and trace element compositions of abyssal peridotites: Implications for mantle melting, melt extraction and post-melting processes beneath mid-ocean ridges. - Journal of Petrology, **45(12),** 2423-2458.

Nordberg, F. E., Fowler, B. A., Nordberg, M. and Friberg, L., Eds. (2007). Handbook of toxicology of metals; Academic Press, Elsevier.

Ogniben, L. (1973). Schema Geologico della Calabria in base ai dati odierni. - Geologica Romana XII, 243– 585.

Pacella, A., Andreozzi, G. B. and Fournier J. (2010). Detailed crystal chemistry and iron topochemistry of asbestos occurring in its natural setting: A first step to understanding its chemical reactivity. - Chemical Geology , **277(3),** 197-206.

Pezzino, A., Angi, G., Fazio, E., Fiannacca, P., Lo Giudice, A., Ortolano, G., Punturo, R., Cirrincione, R. and De Vuono, E. (2008). Alpine metamorphism in the Aspromonte massif: Implications for a new framework for the southern sector of the Calabria-Peloritani orogen, Italy. - International Geology Review, **50(5),** 423-441.

Piccarreta, G. and Zirpoli, G. (1969), Le rocce verdi del Monte Reventino (Calabria). - Bollettino della Societa‘ Geologica Italiana **88 (3),** 469–488.

Piluso, E., Cirrincione, R. and Morten, L. (2000). Ophiolites of the Calabrian Peloritani Arc and their relationships with the Crystalline Basement (Catena Costiera and Sila Piccola, Calabria, Southern Italy). - GLOM 2000 Excursion Guide-Book. Ofioliti **25,** 117– 40.

Piluso, E. and Morten, L. (2004). Hercynian high temperature granulites and migmatites from the Catena Costiera, northern Calabria, southern Italy. Periodico di Mineralogia **73,** 159–72.

Pugnaloni, A., Giantomassi, F., Lucarini, G., Capella, S., Bloise, A., Di Primio, R., and Belluso, E. (2013). Cytotoxicity induced by exposure to natural and synthetic tremolite asbestos: an in vitro pilot study. Acta Histochem. **115(2),** 100–112.

Punturo, R., Fiannacca, P., Lo, G. A., Pezzino, A., Cirrincione, R., Liberi, F., and Piluso, E. (2004). Le cave storiche della “pietra verde” di Gimigliano e Monte Reventino (Calabria): Studio petrografico e geochimico. - Bollettino Della Società Gioenia Scienze Naturali, **37,** 37-59.

Punturo, R., Bloise, A., Catalano, M., Critelli, T., Apollaro, C., Miriello, D., Barrese, E. and Belluso, E. (2013). Asbestos and other fibrous minerals contained in the Gimigliano-Mount Reventino Unit (Calabria Region, Southern Italy). - FIST Geoitalia 2013 – IX Forum Di Scienze Della Terra – Pisa 16-18 Settembre 2013, Epitome 2013, 243.

Spadea, P. (1979). Contributo alla conoscenza dei metabasalti ofiolitici della Calabria settentrionale e centrale e dell’Appennino Lucano. - Rendiconti della Società Italiana di Mineralogia Petrologia, **35,** 251–76.

Spadea, P. (1994). Calabria-Lucania ophiolites. - Bollettino Geofisica Teorica Applicata, **36,** 141–4.

Stanton, M.F., Layard M., Tegeris, A., Miller, E., May, M., Morgan, E. and Smith, A. (1981). Relation of particle dimension to carcinogenicity in amphibole asbestoses and other fibrous mineral. – J. Natl. Cancer Inst. **67,** 965–975.

Suzuki, Y., Yuen, S.R. and Ashley, R. (2005). Short, thin asbestos fibres contribute to the development of human malignant mesothelioma: pathological evidence. - Int. J. Hyg. Environ. Health, **208,** 201–210.

Telloli, C., Malaguti, A., Mircea, M., Tassinari, R., Vaccaro, C., Berico, M. (2014). Properties of agricultural aerosol released during wheat harvest threshing, plowing and sowing. – J. Environ. Sci. (in press).

Vermaas, F.H.S. (1952). The amphibole asbestos of South Africa. - Trans. Geol. Soc. South Africa, **55,** 1-42.

Viti, C., Giacobbe, C. and Gualtieri, A.F. (2011). Quantitative determination of chrysotile in massive serpentinites using DTA: Implications for asbestos determinations. - Am. Mineral. **96,** 1003–1011.

Viti, C. (2010). Serpentine minerals discrimination by thermal analysis. - Am. Mineral. **95,** 631–638.

Zakrzewska, A.M., Capone, P.P., Iannò, A., Tarzia, V., Campopiano, A., Villella, E. and Giardino, R. (2008). Calabrian ophiolites: dispersion of airborne asbestos fibers during mining and milling operations. - Periodico di Mineralogia, **77,** 27-34.

Wicks, F. J., and O'Hanley, D.S. (1988). Serpentine minerals: structure and petrology. – In: Bailey, S. W. (Ed.), Hydrous Phyllosilicates. Rev. Mineral., Min. Soc. Am., **19,** 91-101.